



Contents lists available at ScienceDirect

Journal of Sound and Vibration

journal homepage: www.elsevier.com/locate/jsv

The design of synthesized structural acoustic sensors for active control of interior noise with experimental validation

D.S. Li^a, L. Cheng^{b,*}^a The Goodyear Tire and Rubber Company, Akron, Ohio, USA^b Department of Mechanical Engineering, The Hong Kong Polytechnic University, Hung Hom, Kowloon, Hong Kong

ARTICLE INFO

Article history:

Received 13 June 2008

Received in revised form

4 April 2009

Accepted 2 September 2009

Handling Editor: C.L. Morfey

Available online 3 October 2009

ABSTRACT

In this paper, the feasibility of using synthesized structural acoustic sensors (SSAS) for active noise control inside irregularly shaped enclosures is investigated. A SSAS consists of a cluster of inter-connected discrete PVDF elements, located on the surface of a vibrating structure enclosing a sound field. An optimal design ensures the sensor output to be directly related to the acoustical potential energy inside the enclosure. Hence, synthesized structural acoustic sensors can provide error signals for an active noise control system, and the use of microphones inside the enclosure can be avoided. A cylindrical shell with a floor partition, which can be used to model an aircraft cabin, is used as a test case. PZT actuators are used as control actuators. Both SISO (single input and single output) and MIMO (multi-input and multi-output) control systems are optimally designed using Genetic Algorithms and implemented with a Filtered-X Feedforward LMS (least-mean-square) controller. Their control performances are evaluated with different types of disturbances. To show the effectiveness of the optimal design approach, some non-optimal control systems are also tested and compared with the optimal one. It is shown that with optimally designed SSAS, an active structural acoustic control system can effectively reduce noise inside the enclosures without using any acoustic transducers.

© 2009 Elsevier Ltd. All rights reserved.

1. Introduction

Structure-borne low-frequency noise has always been a major concern. Due to the inefficiency of passive control methods in the case of low-frequency noise, various active control techniques have been investigated in the past decades. According to the type of actuators and error sensors used, active noise control methods can be roughly divided into three categories: The first method involves the use of interior acoustic sources (e.g. loudspeakers) to cancel the noise with the error signal from acoustic sensors (e.g. microphones) [1,2]. The second method employs vibration sources such as shakers [3,4] or surface-mounted piezoelectric actuators [5,6]. As in the first method, the error signal is acquired by acoustic sensors. The third method employs both structural actuators and structural error sensors. Different from the two previous methods, the error signal is provided by structural sensors such as surface-mounted piezoelectric elements. The last option with piezoelectric transducers has many advantages, such as its lightweight and compact features, especially for noise control in aircraft and ground-vehicle cabins due to the space and weight constraints. However, it is far more difficult to realize, because noise may not be attenuated by simply suppressing structural vibration, unless the structural sensors are somehow designed to provide relevant information about the sound field.

* Corresponding author. Tel.: +852 2766 6769; fax: +852 2365 4703.

E-mail address: mmlcheng@polyu.edu.hk (L. Cheng).

The control of sound radiation into a free field using structural sensors has been reported in the literature. Fuller and Burdisso [7] and Wang [8] used a wavenumber domain sensing technique to control sound radiation from a beam. Later on, Maillard and Fuller investigated time domain wavenumber sensing using accelerometers to control noise radiated from a simply-supported plate [9,10] and from a cylinder [11]. Elliott and Johnson [12] conducted theoretical research on controlling sound power radiated from beams and plates into free field using the concept of “radiation mode”. All the work focused on free-field sound radiation from relatively simple structures such as beams, plates, and cylinders.

As far as cavity problems are concerned, however, the intrinsic complexity of structural acoustic coupling makes the problem more challenging, especially when structures with irregular shapes are involved. Snyder and Tanaka [13] studied the active control of sound transmitted into a coupled, rectangular enclosure by shaping structural error sensors according to the shapes of acoustic radiation modes. Cazzolato and Hansen [14,15] conducted research on the control of cavity noise using structural sensors designed based on “radiation modes”. Their research was, however, mainly theoretical. The reported experimental work was limited and inconclusive. Therefore, it is fair to say that the experimental work reported in the literature on the control of noise inside irregularly shaped enclosures without using acoustic sensors is very limited. Considering the fact that most structures in industrial application—such as aircraft cabins—are irregular, and given the strong industrial demand for compact and lightweight noise control technologies, comprehensive investigations on the application of piezoelectric sensors for noise control inside irregularly shaped sound cavities are needed.

This paper presents the design and experimental assessment of synthesized structural acoustic sensors (SSAS) used as error sensors in active control of interior noise inside an irregularly shaped enclosure. It is a continuation of the previously published theoretical work [16–18] on the topic. For completeness, the overall design approach is systematically described in this paper. A synthesized structural acoustic sensor consists of a cluster of inter-connected discrete polyvinylidene fluoride (PVDF) elements. The output of PVDF patches are synthesized to be related to the sound radiating components of the structural vibration. Hence, it can be called “synthesized structural acoustic sensor”. Through optimal design using Genetic Algorithms, synthesized structural acoustic sensors can selectively sense the vibration components significantly radiating sound into the enclosure by filtering out non-critical vibrations. From a slightly different perspective, an optimally designed SSAS sensor can be regarded as a sensor which is able to sense the “acoustic radiation modes” [12–15] for the interior sound field.

Compared with traditional spatial-filter sensors based on structural modal shapes, the developed sensor can be applied to structures with irregular geometry which are common in industry. Compared with microphones, the synthesized structural acoustic sensors are easy to install and non-intrusive to the sound field because PVDF can be easily glued onto the structural surface. Sun et al. [19] presented a concept of global sensor systems for noise control by placing microphones at nodal positions. This concept may be applied to sound cavities with regular geometry excited by tonal or narrow-band sources. From the practical point of view, however, it is inconvenient and sometimes even impossible to place microphones at desired locations inside the sound cavity for many real-world applications.

In this paper, a cylindrical shell with a floor partition is chosen as a test case. Both SISO (single input single output) and MIMO (multiple-input multiple-output) control systems are optimally designed and implemented with a Filtered-X LMS (least-mean-square) Feedforward controller. Their control performances are evaluated with pure tone, multi-harmonic and random sources. The experimental results indicate that the control technology with synthesized structural acoustic sensors is not only effective for pure-tone sources but also for multi-harmonic and broadband random noise sources. The control performances of the optimal control systems are also compared with those of non-optimal configurations, showing the superiority of optimally designed synthesized structural acoustic sensors in terms of sound reduction.

2. Structural-acoustic model of a cylindrical shell with a floor partition

The structure to be considered in the present research consists of a thin, finite, circular cylindrical shell with a longitudinal floor partition, as shown in Fig. 1. Both the shell and the floor are assumed to be homogeneous and isotropic. The shell-floor structure is simply-supported at the two ends. As far as the acoustic boundary condition is concerned, the shell wall and the floor are assumed to be flexible, while the two end plates are assumed to be acoustically rigid. The cavity of interest is the space above the floor. The model has been detailed in the previous work [16]. For the sake of completeness, it is briefly summarized here.

The Rayleigh–Ritz method is used to develop the structural model [20]. The displacements of the shell and of the floor are decomposed on the basis of the natural modes of a plain, cylindrical shell and a floor, respectively. Structural coupling between the shell and the floor is modeled using an artificial spring system [21] for every permitted degree of freedom at the shell–plate junction. The stiffness of all springs is assumed to be uniformly distributed along the two shell–floor junctions.

The sound field is modeled using the Integro–Modal approach [22], which was developed for analyzing the acoustic properties of irregular cavities, for which it is not possible to apply the technique of separation of variables. An irregularly shaped enclosure is handled as a multi-connected cavity system, with either regular or slightly irregular sub-volumes. A virtual membrane separates each pair of adjacent sub-cavities. An integral formulation ensures global continuity of the pressure between adjacent sub-cavities by assigning a zero-mass and zero-stiffness to the membrane. The cavity is discretized into N sub-cavities of both regular and irregular shapes. The modal characteristics of regular sub-cavities are

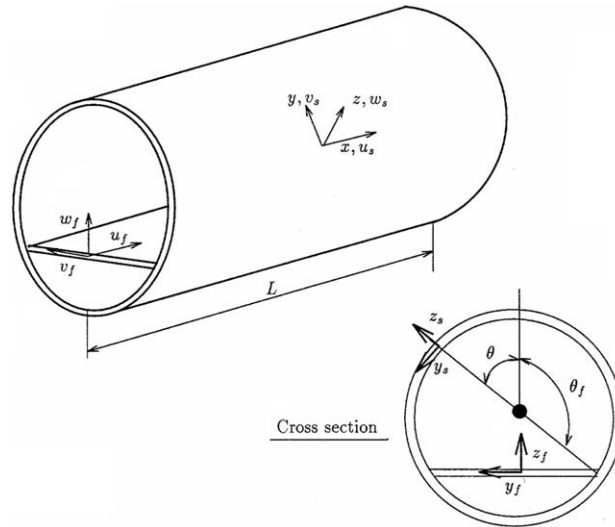


Fig. 1. Schematic drawing of test structure and coordinate system.

analytically available for performing sound-pressure decomposition. For irregular sub-cavities, the modes of the bounding sub-cavities (called the envelope), which are chosen to be of regular shape, are used to perform the pressure decomposition and to obtain the Green's function.

The above treatment leads to a unified structural-acoustic model, which can be expressed as:

$$\begin{bmatrix} \mathbf{K}_{SS}(\omega) & \mathbf{K}_{SF} \\ \mathbf{B}_{FS}(\omega) & \mathbf{A}_{FF}(\omega) \end{bmatrix} \begin{Bmatrix} \mathbf{U}^S \\ \mathbf{P} \end{Bmatrix} = \begin{Bmatrix} \mathbf{F}_{SS} \\ \mathbf{0} \end{Bmatrix} \quad (1)$$

where \mathbf{K}_{SS} is the dynamic stiffness matrix of the structural system; \mathbf{K}_{SF} is the fluid-structure coupling matrix; \mathbf{B}_{FS} is the matrix obtained using various coefficients of the acousto-elastic coupling. \mathbf{U}^S and \mathbf{P} are, respectively, the unknowns related to the structural components and acoustic vectors. \mathbf{A}_{FF} contains the acoustic mass and stiffness matrices. \mathbf{F}_{SS} is the vector related to the mechanical excitation force applied to the structure.

Control actions generated by PZT actuators can be incorporated into the above model using relatively simple models. Each PZT actuator pair consists of two PZT pieces attached on the opposite sides of the shell. Two options are available [23]. One is the bending model, simulating the effect of two PZT pieces operating out of phase. The other is the in-plane force model, simulating the effect of two PZT pieces operating in-phase. It was found that, for cylindrical-shell structures, the in-plane force model provides better sound reduction than the bending model and should be used for the control of noise inside a cylindrical-shell structure [17]. Therefore, the in-plane force model is adopted here, with details provided in [17].

3. Optimal design approach for synthesized structural acoustic sensors

An effective control system requires the optimal design of both actuator and sensor configurations. The optimal design of PZT actuators has been fully discussed in previous work [17]. The following discussion will focus more on the sensor design.

As is known, the sound radiation efficiency of different structural modes varies. Hence, the acoustic potential energy inside the enclosure does not necessarily correlate with the total vibration energy of the structure. As a result, the interior noise may not be attenuated by simply suppressing structural vibration. To replace acoustic sensors with structural sensors in an active noise control system, the structural sensors must only (or at least mainly) sense the structural modes significantly radiating sound into the enclosure instead of measuring any vibration. The key is how to design this kind of structural sensors.

A synthesized structural acoustic sensor developed in the research consists of a cluster of discrete PVDF elements as illustrated in Fig. 2. The discrete elements can be anywhere on the structural surface and they are connected by wires, providing a great capability for sensing critical vibration modes and flexibility for sensor installation. The output of a synthesized structural acoustic sensor is the sum of the output of all the elements, expressed as:

$$V = \sum_{i=1}^n V^i \quad (2)$$

where V^i is the output of the i th element and n is number of elements. When PVDF is used on the surface of a cylindrical-shell structure, and on the assumption of a prominent out-of-plane displacement and negligible temperature effect, the output of a PVDF element in Eq. (2) can be expressed as [24]:

$$V^i = \frac{h_s e_{31}}{\varepsilon_{33} A} \int \int_A \left[\frac{w}{R} - \frac{h_s + h_c}{2} \left(\frac{\partial^2 w}{\partial x^2} + \frac{\partial^2 w}{R^2 \partial \theta^2} \right) \right] R dx d\theta \quad (3)$$

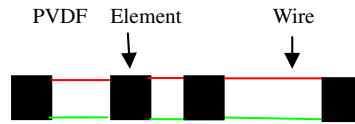


Fig. 2. Diagram of a synthesized structural acoustic sensor.

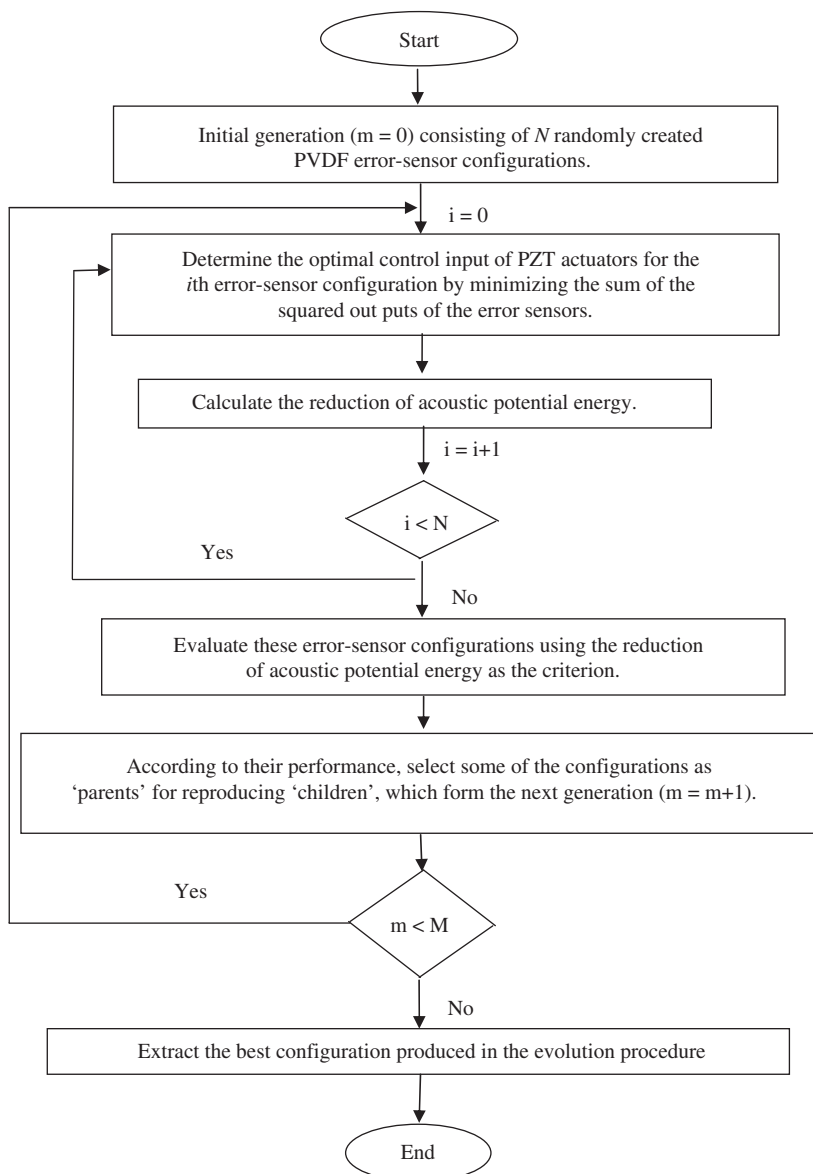


Fig. 3. Design process of synthesized structural acoustic sensors.

with h_s being the thickness of PVDF, e_{31} the piezoelectric material constant, ϵ_{33} the permittivity constant, A the surface area of the PVDF element, h_c the thickness of the cylindrical shell, R the curvature radius of the cylindrical shell, x the longitudinal coordinate, θ the circumferential coordinate, and w the radial displacement of the cylindrical shell.

Genetic Algorithms (GAs) are used to design the synthesized structural acoustic sensors. During the optimal design process, GAs explore a large number of possible sensor configurations by varying the size, the number and the locations of elements. For each searched sensor configuration, the optimal control input of the PZT control actuators is determined by minimizing the sum of the squared outputs of the error sensors, as an actual LMS controller does. The cost function used to evaluate the searched sensor configuration is the reduction of the acoustical potential energy in the enclosure. The sensor configuration providing higher acoustical potential energy reduction has a higher possibility of “surviving” during the evolution process and producing “children”. Hence, at the end of the design process, one can find an optimal sensor configuration where minimization of the sensor outputs results in the greatest attenuation of the interior acoustic potential energy. The whole process is illustrated in Fig. 3.

The usage of the reduction of acoustical potential energy as the cost function in the design guarantees the sound reduction achieved with the designed sensors as significant as possible. The designed sensors have the capability to selectively measure the vibration components significant radiating sound into the enclosure and can be used as error sensors for active noise control. When a control system minimizes the error signals (i.e., the measured vibration), the radiated noise will be reduced because its source is suppressed.

In our previous work [18], the control performance of synthesized structural acoustic sensors designed using the approach was compared with that achieved by minimizing the acoustic potential energy in the sound cavity. It was found that at the design frequency, the achieved sound reductions are very close, and that when the excitation frequency deviates from the design frequency, significant sound reduction can still be achieved with the sensors at most frequencies in the low-frequency range.

4. Design of SISO and MIMO control systems

The dimensions and material properties of the structure used in the simulations and experiments are as follows: the cylindrical shell is 1.168 m long, 0.504 m in internal diameter and 0.0032 m thick. The floor is rigidly connected to the shell at an angle θ_f of 131° . The whole structure is made of steel with a density 7860 kg/m^3 , Poisson ratio 0.3 and Young's modulus $2.07 \times 10^{11} \text{ N/m}^2$.

One PZT actuator at $(0.31 \text{ m}, 90^\circ)$ is used as a disturbance source to excite the structure. Due to the curvature effect of cylindrical-shell structures, the PZT actuator can actually generate a bending motion. Control is also provided by PZT actuators with the same size and properties. The size of each PZT patch is 50.8 mm long by 20 mm wide by 0.508 mm thick. The thickness of PVDF is $5.2\text{E-}05 \text{ m}$, with a permittivity constant $106\text{E-}12 \text{ F/m}$ and a piezoelectric constant $9.6\text{E-}03 \text{ C/m}^2$. The size of each PVDF element is 0.17 m long by 0.02 m wide.

In the design, to avoid having a control actuator too close to, or even overlapping with, the disturbance source, a clearance distance between the disturbance and a control actuator, which is 0.05 m in the longitudinal direction or 10° in the circumferential direction, is imposed. Overlapping among the control PZT actuators is avoided using the forced-mutation method. The design space is the shell surface.

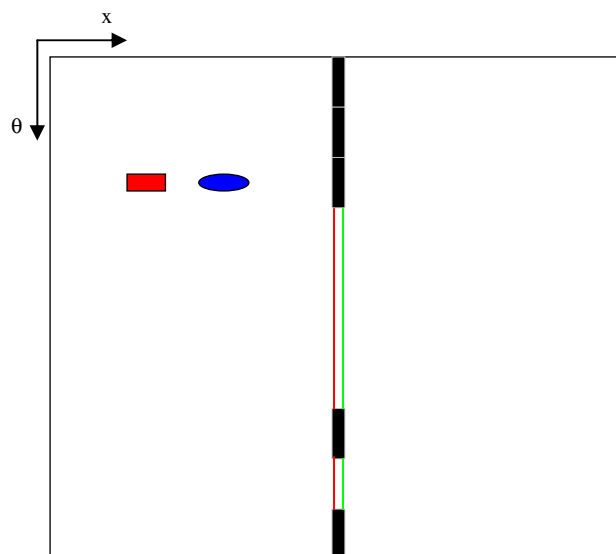


Fig. 4. Optimal configuration of a SISO control system (Control system1) ■ disturbance, ● control actuator, and ■ SSAS sensor.

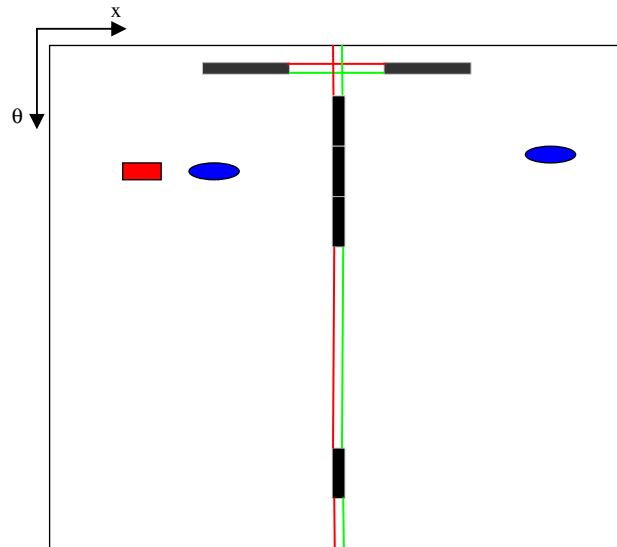


Fig. 5. Optimal MIMO (2×2) control system (Control system 5) ■ disturbance, ● control actuator, and █ SSAS sensor.

SISO and MIMO (2×2) systems are optimally designed to target the acoustic resonance frequency of 297 Hz. Fig. 4 shows the optimal configuration of the SISO control system. To facilitate the illustration, the shell surface is cut along the longitudinal direction at $\theta=0^\circ$, and stretched into a plane surface in the figures. The small rectangle represents the disturbance actuators, the small ellipse denotes the control actuator (actually the control actuator is a rectangular plate with the same size as the disturbance actuators), and PVDF elements are represented by large black rectangles. The optimal position of the PZT actuator is $(0.42 \text{ m}, 90^\circ)$, which was determined following the methodology discussed in [17]. The longitudinal position of the PVDF sensor on the structural surface is $x=0.6 \text{ m}$. The previous investigation [18] has shown that more sound reduction can be achieved with a circumferential strip-typed SSAS sensor than with a longitudinal strip-typed SSAS sensor in a SISO control system because for cylindrical-shell structures, the circumferential modes play a key role in sound radiation into the enclosure due to a much stronger coupling of the circumferential modes to the interior sound field than the longitudinal modes in the low frequency range. Therefore, in a SISO control system, a circumferential SSAS sensor is preferable to be used for a cylindrical-shell structure.

Similarly, Fig. 5 shows the optimally designed MIMO (2×2) control system. The optimal control actuators are located at $(0.42 \text{ m}, 90^\circ)$ and $(0.91 \text{ m}, 79^\circ)$. The longitudinal position of the sensor along the circumferential direction is 0.6 m , and the circumferential position of the sensor along the longitudinal direction is 10° . These two systems will be implemented and tested in the following experimental investigations.

5. Experimental investigations and analyses

5.1. Experimental setup

Experimental studies were conducted to validate the effectiveness of the two systems designed above. The test structure has the same dimensional and material properties as that used in the design. The floor was welded to the inner shell skin. Two steel end caps of 0.0254 m thick were used to form the rigid acoustic boundaries.

The experimental setup is shown in Fig. 6. In the figure, PC 1 was employed as the platform for the Filtered-X Feedforward LMS controller [25] and as the signal generator providing the disturbance signal. Two cascade second-order (cut-off frequency 1000 Hz) Chebyshev filters were used as anti-aliasing filters for the input and output signals. The data were acquired and saved for post-processing in PC 2. The sampling frequency was 2000 Hz . The frequency range of interest was below 500 Hz .

The sound field was measured using two $\frac{1}{2}$ " pre-polarized condenser microphones mounted on a movable traverse at non-dimensional radial locations $r/a=0.19$ and 0.56 with r the radial coordinate of the microphones and a the radius of the cylindrical shell. For each test, sound was measured at 12 points in the cavity tabulated in Table 1. The measurement position is denoted by three indices $(x, \theta, r/a)$ with x the longitudinal coordinate, θ the circumferential coordinate, and r/a the non-dimensional radial location. The average of the power spectral density (PSD) of the microphone signals at the 12 measurement locations was used to represent the global sound field. The control performance of a control system was measured by the difference between the average PSD before and after control. It should be pointed out that the microphones were not part of the control system and are not needed in a real-life application. They were used here to measure the performance of a control system.

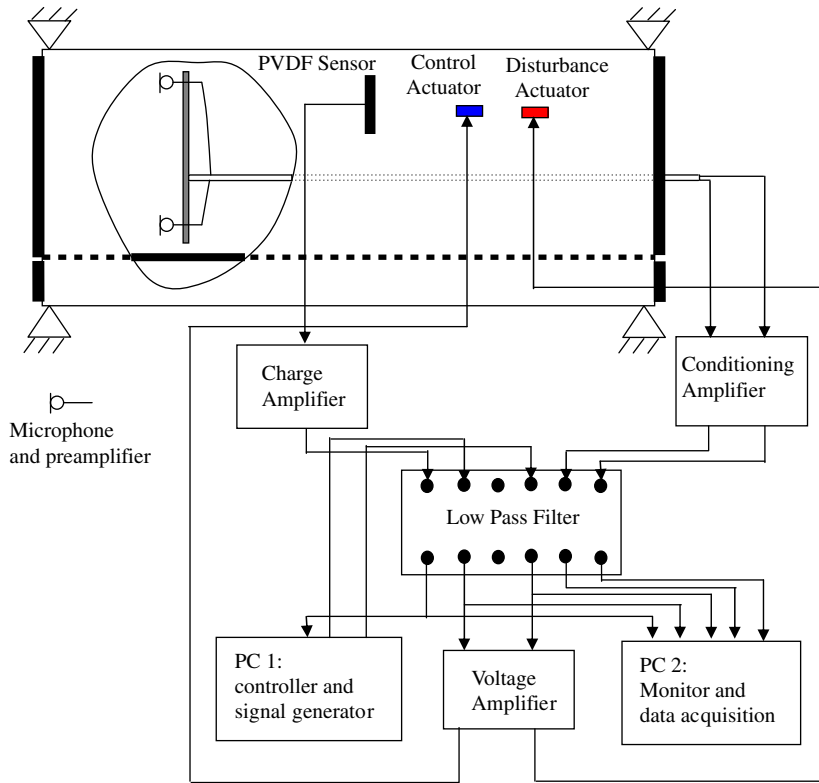


Fig. 6. Schematic drawing of experimental setup.

Table 1
Sound measurement positions.

(0.2567 m, 0°, 0.56)	(0.2567 m, 180°, 0.19)	(0.2567 m, 90°, 0.56)	(0.2567 m, 270°, 0.19)
(0.5567 m, 0°, 0.56)	(0.5567 m, 180°, 0.19)	(0.5567 m, 90°, 0.56)	(0.5567 m, 270°, 0.19)
(0.8567 m, 0°, 0.56)	(0.8567 m, 180°, 0.19)	(0.8567 m, 90°, 0.56)	(0.8567 m, 270°, 0.19)

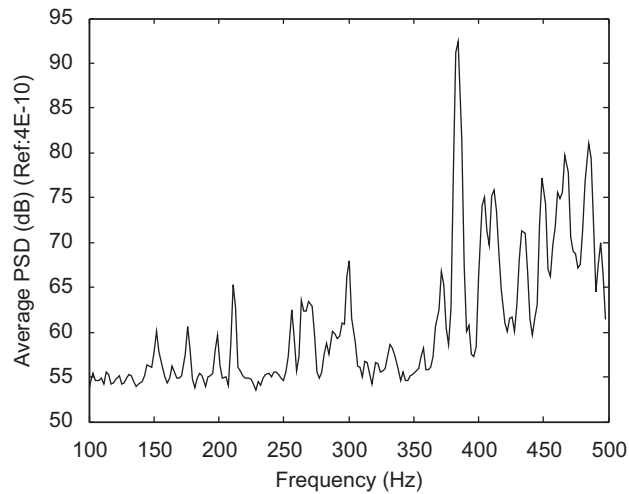


Fig. 7. PSD of the enclosed sound field excited by a random vibration source.

The averaged PSD of measured sound-pressure signals in the sound cavity excited by a random vibration source is given in Fig. 7. Since there are no acoustic and structural modes below 100 Hz, the frequency range shown in the figure starts from 100 Hz. Some peaks are dominated by acoustic modes such as those at 150, 300, 380, 408, 450, 460 and 483 Hz. The others are either structural modes or coupled modes. The acoustic resonance frequency of 300 Hz of the experimental structure corresponds to the design frequency of 297 Hz in the numerical simulations.

5.2. Experimental results and analyses

Six control systems listed in Table 2 were implemented, tested and compared. The structure was excited to vibrate by a PZT actuator attached to the cylindrical-shell surface. Control system 1 was the optimal SISO system shown in Fig. 4. Control system 5 was the optimal MIMO system shown in Fig. 5. The other four configurations have non-optimal sensors.

5.2.1. Control performance of an optimal SISO control system

Fig. 8 shows the real-time control signals, output signals from the error sensor and from the microphones at (0.5567 m, 0°, 0.56) and (0.5567 m, 180°, 0.19) where strong sound fields exist when the structure was excited at the acoustic resonance frequency of 300 Hz. From this figure, one can observe that when the output of the error sensor was minimized, the sound pressure at the measuring positions was also significantly reduced. Both the vibration and sound-field signals converged quickly and stably after the control was applied; for the vibration signal, the convergence time was only around 0.2 s, for the sound signal, it converged within about 0.7 s. Fig. 9 shows the average PSD of the sound pressures at all of the measurement positions, where the solid line represents the average PSD before control and the dashed line denotes that after control. As can be seen from Fig. 9, up to 10 dB of sound reduction is achieved at the acoustic resonance frequency of 300 Hz. It should be noted that the overall sound reduction is not as high as the reduction of the error signal. This is because

Table 2

Control systems implemented in the experiments.

No.	PZT actuator	SSAS sensor	Control channels
1	Optimal	Optimal	SISO
2	Optimal	Non-optimal	SISO
3	Optimal	Non-optimal	SISO
4	Optimal	Non-optimal	SISO
5	Optimal	Optimal	MIMO
6	Optimal	Non-optimal	MIMO

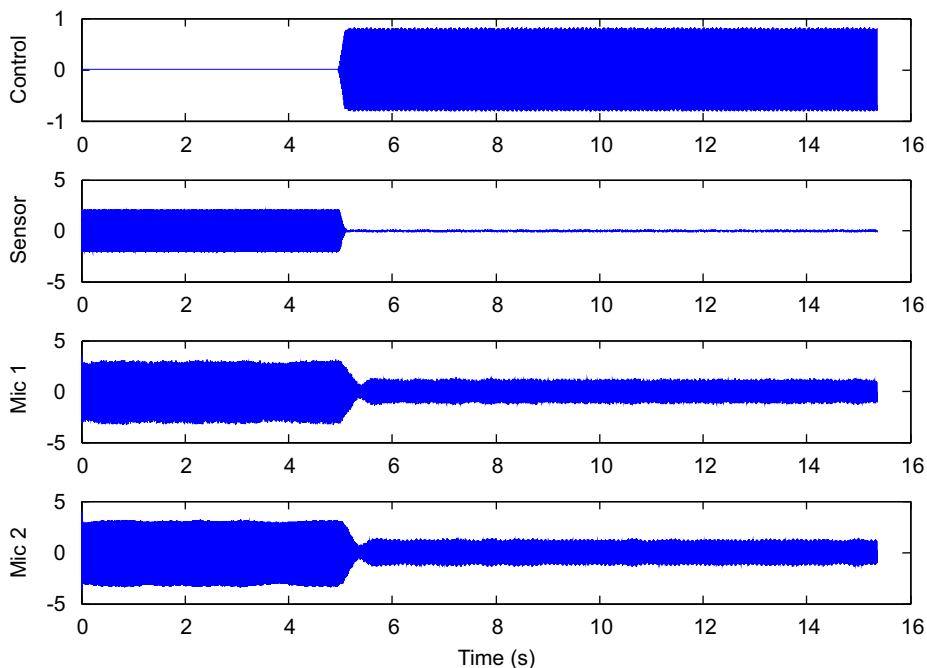


Fig. 8. Real-time signals of the optimal SISO control system (excitation frequency 300 Hz).

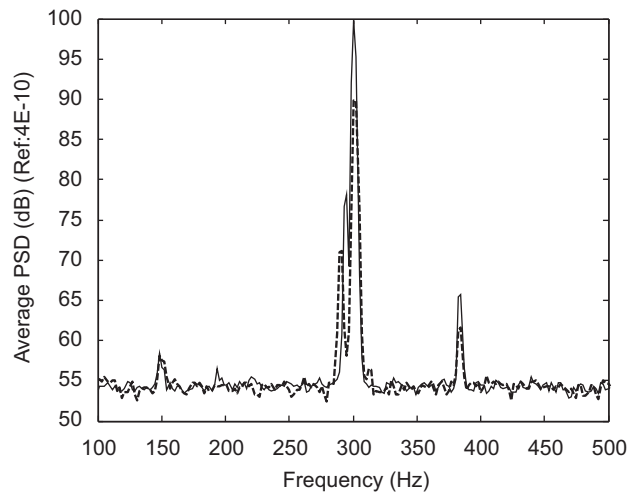


Fig. 9. Global control performance of the optimal SISO system (excitation frequency 300 Hz) — before control, - - - - - after control.

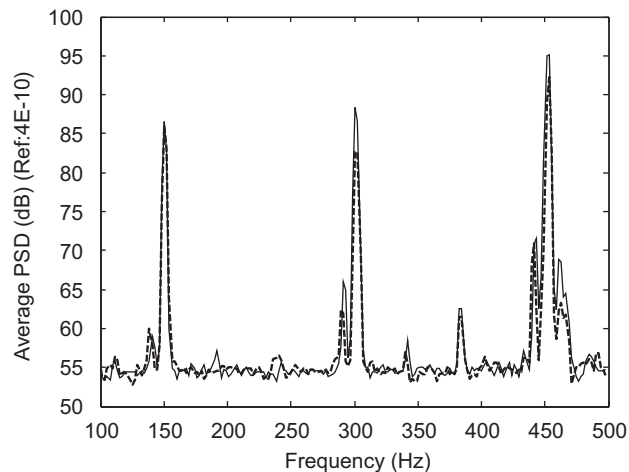


Fig. 10. Global control performance of the optimal SISO system for a multi-harmonic disturbance source — before control, and - - - - - after control.

a single sensor may not be able to sense all the structural modes radiating sound into the cavity considering the complexity of the structural acoustic system with irregular geometry. The sensor design method, however, does make sure that the most significant structural modes in terms of sound radiation are first sensed with the sensing resources available. Therefore, even with a single synthesized structural acoustic sensor, a significant sound attenuation can still be achieved.

If a control system is only effective at the design frequency, the application would be limited. Therefore, tests were also conducted at other acoustic and structural resonance frequencies under 500 Hz. The experimental results show that the optimal control system has a good control performance not only at the design frequency but also over the full low-frequency range. For example, at the acoustic resonances of 450 and 483 Hz, the global sound reductions were 5.8 and 8.8 dB, respectively; at the structural resonance frequency of 176 Hz, a 7.2 dB sound reduction was achieved.

More complex disturbances were then tested. Fig. 10 shows the control performance when the structure was excited by a multi-harmonic excitation with a fundamental frequency of 150 Hz. There was no sound attenuation at 150 Hz. The 6 and 3 dB sound reductions were achieved at 300 and 450 Hz, respectively. The sound reductions were less than those achieved when the structures were excited with single-frequency signals, indicating the limited capability of a SISO control system for attenuating multi-harmonic noise. To achieve better sound attenuation performance, a MIMO control system is needed.

Fig. 11 shows the interior sound reduction when the structure was excited by a random vibration source. As is observed, apparent sound attenuation is achieved at many acoustic and structural natural frequencies. For example, the sound

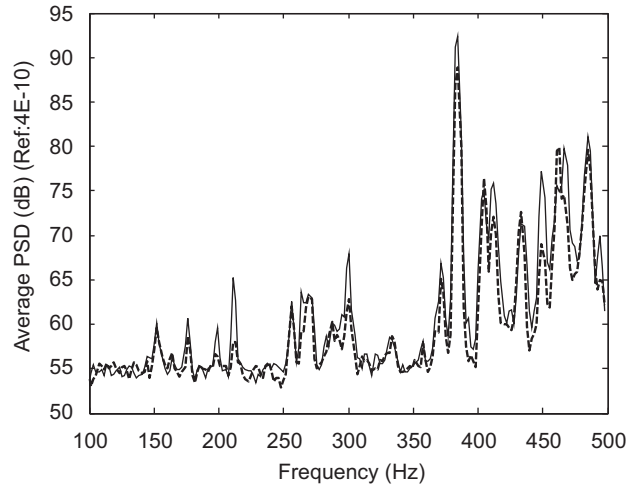


Fig. 11. Global control performance of the optimal SISO system for a random disturbance source. — Before control, - - - - after control.

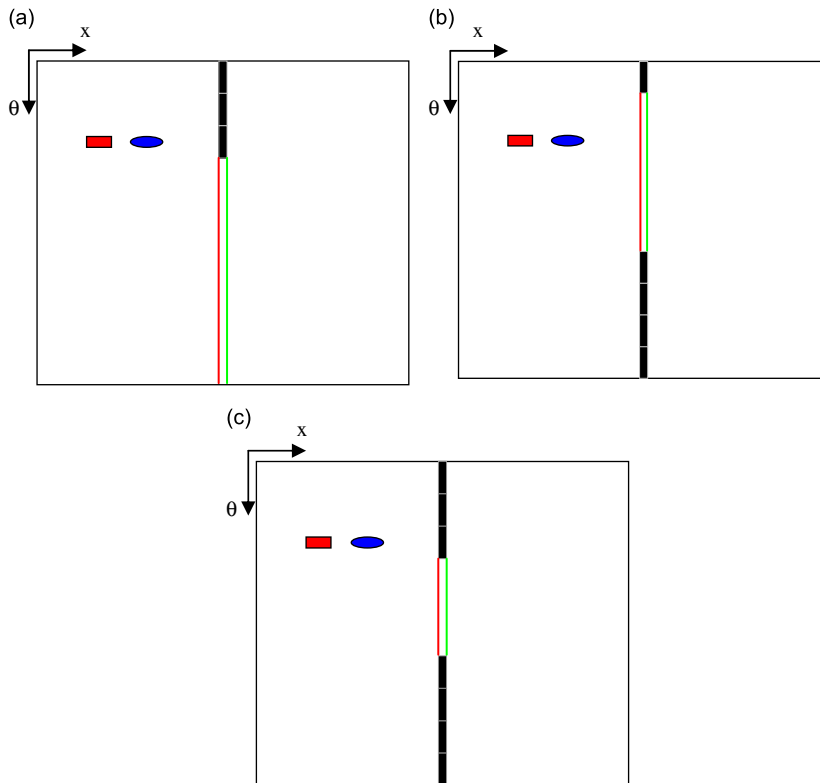


Fig. 12. SISO control systems with non-optimal sensors: (a) Control system 2, (b) Control system 3, (c) Control system 4 ■ disturbance, ● control actuator, and SSAS sensor.

reduction is 4 dB at the acoustic natural frequency of 380 Hz, at which the strongest sound exists. Even though no sound reduction is achieved at some frequencies, no obvious “spillover” happens. Hence, the overall sound is attenuated as a result of control. It should be noted that a feedforward controller is typically less effective in controlling broadband random disturbance [25].

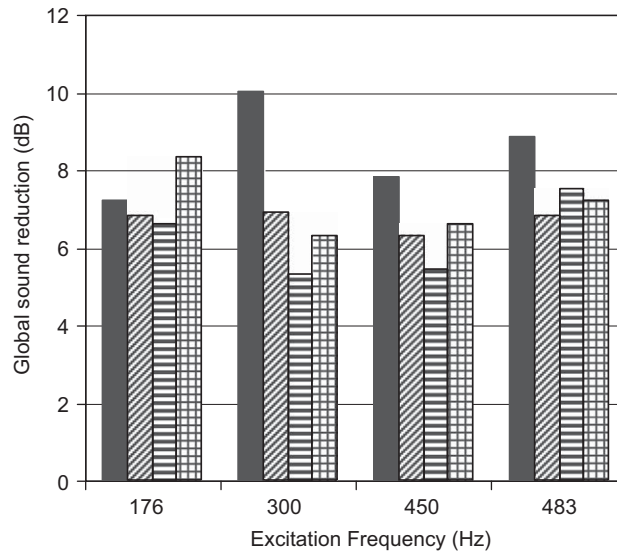


Fig. 13. Comparison of the global sound reduction achieved by the optimal control system and by the three systems with non-optimal sensor optimal Control system 1, non-optimal Control system 2, non-optimal Control system 3, and non-optimal Control system 4.

5.2.2. Performance comparison of optimal and non-optimal error sensors

To validate the effectiveness of the optimal design of error sensors, the optimal SISO control system was compared with three other non-optimal SISO control systems (Fig. 12) consisting of the same optimal control actuator and non-optimal error sensors.

The non-optimal error sensor in Control system 2 (Fig. 12a) was implemented by removing two PVDF elements from the optimal error sensor in Fig. 4. The error sensor in Control system 3 (Fig. 12b) was obtained by re-arranging the position of the PVDF elements of the optimal sensor. By adding two PVDF elements to the optimal sensor, the error sensor in Control system 4 (Fig. 12c) was created. The global sound reductions achieved by these control systems are shown in Fig. 13. From this figure, one can observe that, at all of the acoustic resonance frequencies, the control system with an optimal sensor had better control performance. At the design frequency of 300 Hz, the improvement was over 3 dB compared to the best reduction achieved by the three non-optimal control systems. At the structural frequency of 176 Hz, both the optimal and non-optimal systems achieved considerable sound attenuation.

Since everything was the same in all of these systems except the error sensor, one can conclude that the performance difference was due to the error sensor configurations. Different configurations of error sensors may result in their different abilities to sense the structural modes critical for the sound radiation and to filter out non-critical vibration modes. In this regard, the transfer function between the control actuator and the error sensor provides interesting information. The transfer function in the optimal SISO system (Fig. 14a) shows that the optimal error sensor has a strong ability to sense the structural modes, such as the modes at 200 and 264 Hz. The structural acoustical coupling analysis [16] indicates that these structural modes have high radiation efficiency. The transfer function of Control system 2 with a non-optimal sensor is shown in Fig. 14(b). Comparing Figs. 14(a) and (b), one can clearly see that the ability of the non-optimal error sensor to observe the low-frequency structural modes with high radiation efficiency was weak, resulting in an inefficient control over these structural modes. Hence, the sound reduction achieved by the non-optimal control system was less than that achieved by the optimal control system. The same observation can be made from the transfer functions of Control systems 3 and 4.

Fig. 15 shows the control performance of the three non-optimal sensors when the structure was excited by a multi-harmonic vibration source with a fundamental frequency of 150 Hz. As can be observed, 2–3 dB of sound reduction was achieved at 300 Hz for all of the three non-optimal configurations. At 150 Hz, some “spillover” was observed. At 450 Hz, the sound was barely attenuated.

In the optimal SISO control system, the error sensor consisted of 5 PVDF elements. Control systems 2 had 3 PVDF elements, while Control systems 3 and 4 had 5 and 7 elements, respectively. The experimental results in Figs. 13 and 15 show that the coverage rate of PVDF film over the structure is not a determinant factor influencing the noise control performance, in agreement with the observations made in the numerical investigation [18].

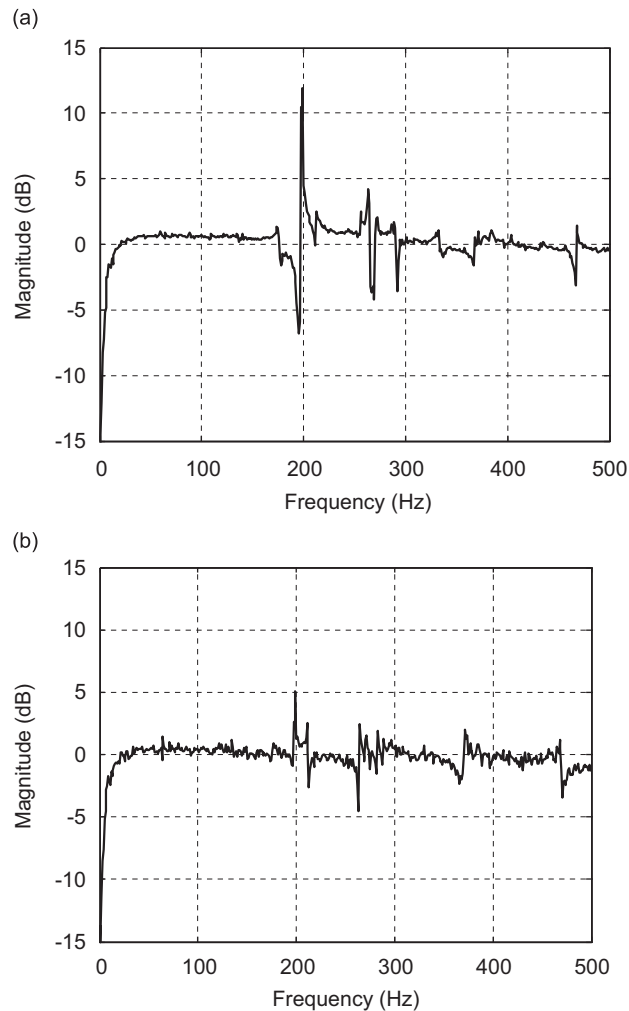


Fig. 14. Transfer functions between the control actuator and the error sensor: (a) Control system 1 with optimal sensor, and (b) Control system 2 with non-optimal sensor.

5.2.3. Control performance of MIMO control systems

In addition to the SISO control systems, the optimal MIMO (2×2) control system shown in Fig. 5 was also implemented and tested. Fig. 16 shows the real-time control and error sensor signals and the signals from the monitoring microphones at 300 Hz. It shows that the control system converged fast and stably when the control was applied. As is shown in Fig. 17, the optimal 2×2 control system achieved much higher sound reduction than the optimal SISO system did. For example, at the design frequency, the global sound reduction achieved by the 2×2 control system was 5.8 dB higher than that achieved by the optimal SISO system. By increasing the number of synthesized structural acoustic sensors, one increased the control system's capability of sensing more radiation modes with significant sound radiation. As a result, higher sound reduction was achieved with two synthesized structural acoustic sensors.

Fig. 18 shows the control performance of the optimal 2×2 system for a multi-harmonic disturbance source. It can be observed that the sound was significantly attenuated at all the three major frequencies 7, 16 and 12 dB of sound reductions were achieved at 150, 300 and 450 Hz, respectively. Note that the SISO control system failed to control the peak at 150 Hz, as illustrated in Fig. 10. The results show that, with a MIMO system, much better sound reduction can be achieved, especially for a multi-harmonic noise source.

The experimental results of SISO and MIMO control of a multi-harmonic noise source can be explained by observing the structural acoustic coupling characteristics of cylindrical-shell structures [16]. A structural mode couples with an acoustic mode only when their longitudinal orders are an odd-even combination pair. The longitudinal orders of acoustic modes at 150, 300 and 450 Hz are 1, 2 and 3, respectively. Therefore, the structural modes coupling with the acoustic mode at 300 Hz have odd longitudinal orders while those coupling with the acoustic modes at 150 and 450 Hz have even longitudinal orders. The circumferential SSAS sensor, optimally designed at 300 Hz, is located close to the longitudinal

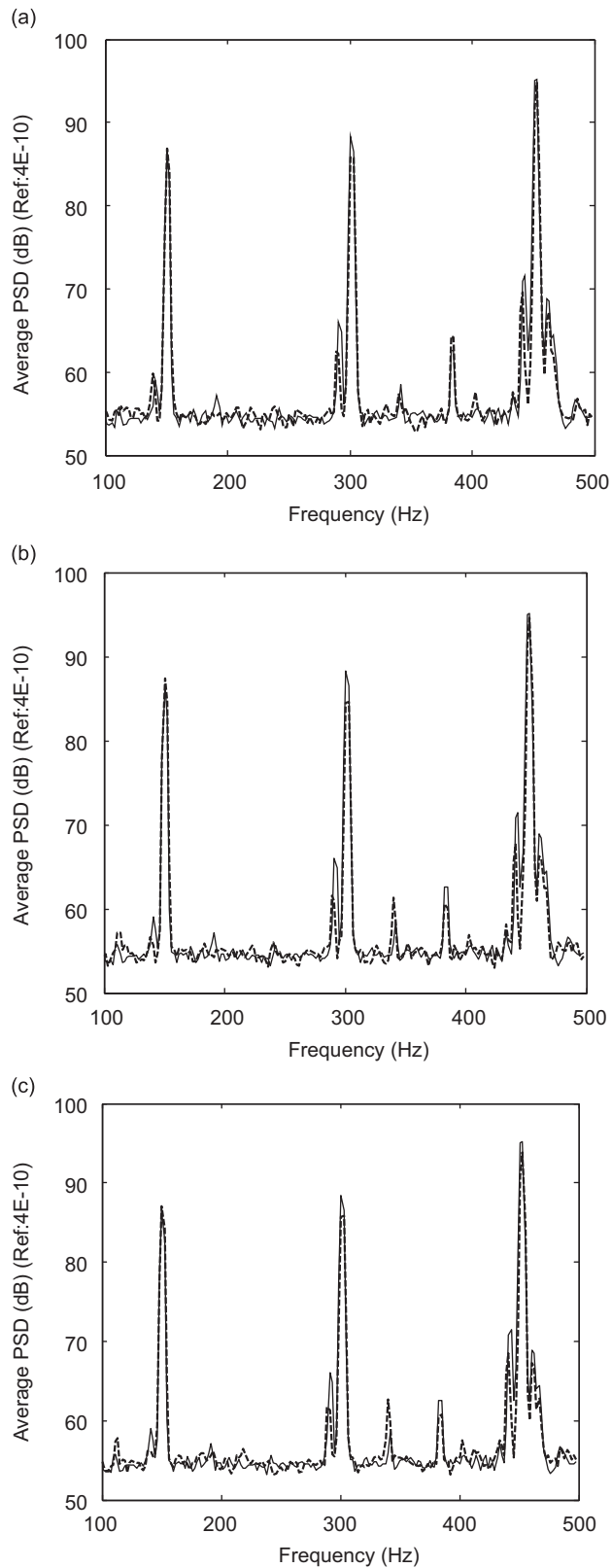


Fig. 15. Control performance of the three control systems with non-optimal sensors for a multi-harmonic disturbance source: (a) Control system 2, (b) Control system 3, and (c) Control system 4.

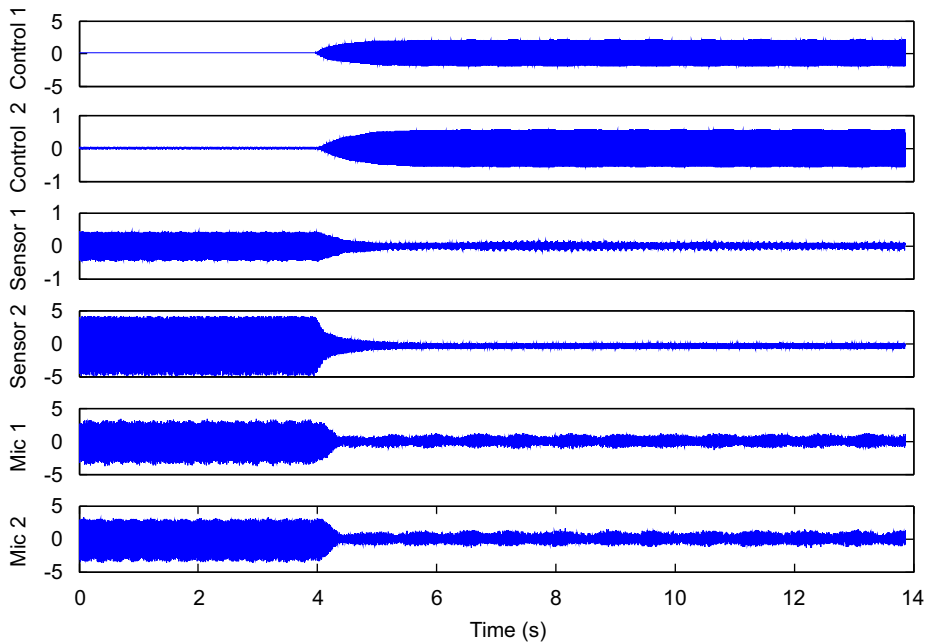


Fig. 16. Real-time signals of the optimal MIMO (2 × 2) system.

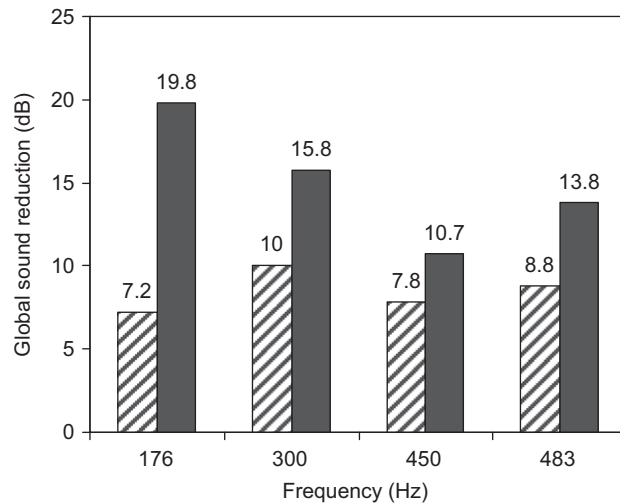


Fig. 17. Comparison of the global sound reduction achieved by the optimal SISO and the optimal MIMO (2 × 2) systems 1 × 1, 2 × 2.

center of the cylindrical-shell structure, which is the anti-node position of structural modes with odd longitudinal orders, and the node position of structural modes with even longitudinal orders. Hence, the circumferential SSAS sensor has a strong capability to observe structural modes with odd longitudinal orders coupling with the 300 Hz acoustic mode, and very limited capability to sense structural modes with even longitudinal orders coupling with the acoustic modes at 150 and 450 Hz. Therefore, with the SISO control system, small or no sound reductions were achieved at 150 and 450 Hz. The MIMO control system has a longitudinal SSAS sensor, which can sense the structural modes with both even and odd longitudinal orders. Hence, with the MIMO control system, significant sound reductions were achieved at all the three harmonic frequencies.

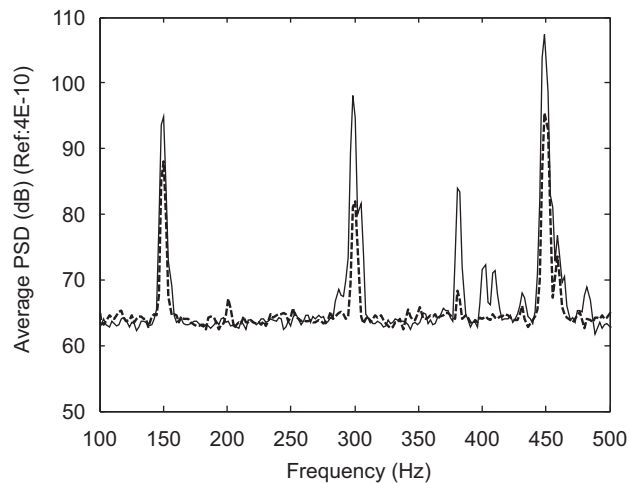


Fig. 18. Global control performance of the optimal MIMO (2×2) system for a multi-harmonic disturbance source — before control, - - - after control.

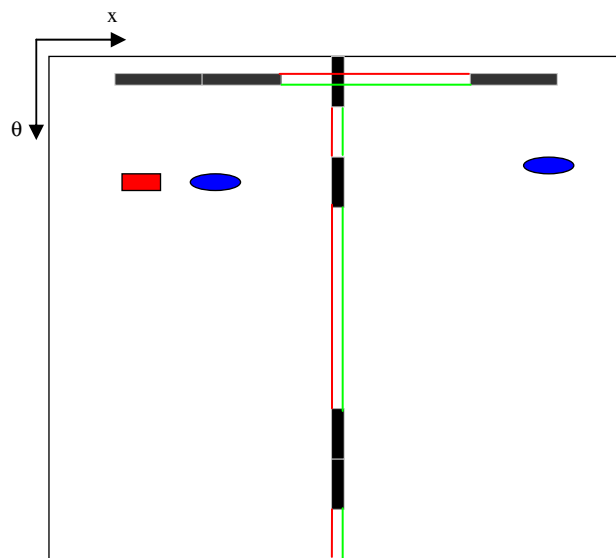


Fig. 19. A MIMO (2×2) control system with non-optimal sensors — disturbance, — control actuator, and — SSAS sensor.

The performance of the optimal MIMO control system was also compared with that of a non-optimal MIMO control system (Fig. 19) with a pure-tone disturbance source. As can be seen, both optimal and non-optimal configurations have basically the same coverage area, with only slightly different arrangements. However, as shown in Fig. 20, the global sound reduction achieved by the optimal system is 13.2 dB higher than that achieved by the non-optimal system at the design frequency. At other frequencies, much better performance of the optimal MIMO system is also observed. For a MIMO control system, the performance improvement through optimal design is more significant than for a SISO control system. From here, one can see the great benefit of this optimal design approach in MIMO control.

To test the sensor robustness, the optimal SISO and MIMO control systems were tested with two sets of optimal sensors at the optimal location. The experimental results repeated well.

6. Conclusions

The feasibility of using synthesized structural acoustic sensors (SSAS) for active noise control inside irregularly shaped enclosures is experimentally investigated in this paper. The sensor consists of a cluster of PVDF elements, with their output synthesized to be related to the sound radiating components of the structural vibration.

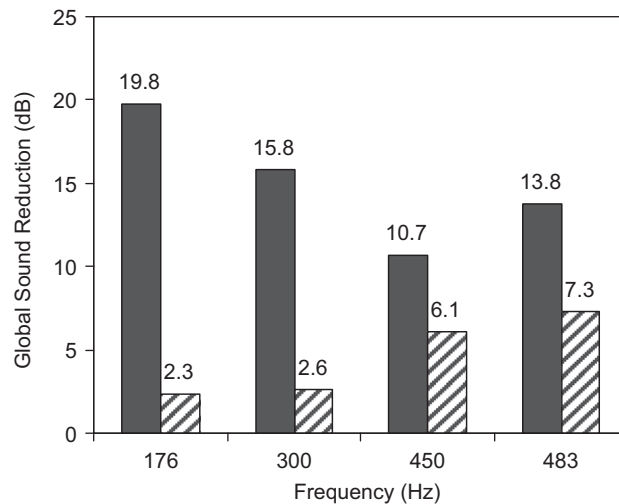


Fig. 20. Comparison of the global sound reduction achieved by the optimal 2×2 system (Control system 5) and by the non-optimal 2×2 control system (Control system 6) ■ optimal, and ▨ non-optimal.

Synthesized structural acoustic sensors are designed using Genetic Algorithms. The reduction of acoustical potential energy in the enclosure was used as the cost function, which guarantees a significant sound reduction with the optimal SSAS sensors. The synthesized structural acoustic sensors can selectively sense the vibration components significantly radiating sound into the enclosure instead of any structural vibration. Hence, synthesized structural acoustic sensors can be used to replace microphones in an active noise control system as error sensors. One of the biggest advantages of using synthesized structural acoustic sensors as error sensors is that global control can be achieved. An active noise control system with synthesized structural acoustic sensors and PZT control actuators is compact, lightweight and non-intrusive to the enclosed sound field, which are very attractive features for industrial applications.

Optimal SISO and MIMO control systems were designed and implemented with a Filtered-X Feedforward LMS controller. Their control performances were evaluated for different types of disturbance sources ranging from pure-tone and multi-harmonic to broadband random sources. The experimental results indicated that, with optimal design, a control system with SSAS can effectively reduce sound inside enclosures not only for relatively simple pure-tone disturbance sources but also for multi-harmonic and random sources to a certain extent in the low-frequency range under 500 Hz. For complex disturbance sources such as multi-harmonic, MIMO control is needed to achieve significant sound reduction. The benefit gained from this design approach is even more pronounced for MIMO control systems.

The general methodology proposed in this paper can work for enclosures with either regular or irregular geometries. It is especially appealing when irregularly-shaped structures are involved because, in this case, traditional sensors and design methods based on modal information are no longer effective.

Acknowledgments

Supports from the Central Research Grant of The Hong Kong Polytechnic University G-YG19 and G-U553 are acknowledged.

References

- [1] A.J. Bullmore, P.A. Nelson, S.J. Elliott, Theoretical studies of the active control of propeller-induced cabin noise, *Journal of Sound and Vibration* (1990) 191–217.
- [2] A.J. Bullmore, P.A. Nelson, S.J. Elliott, In flight experiments on the active control of propeller-induced cabin noise, *Journal of Sound and Vibration* 140 (2) (1990) 219–238.
- [3] M.A. Simpson, T.M. Luong, C.R. Fuller, J.D. Jones, Full-scale demonstration tests of cabin noise reduction using active vibration control, *Journal of Aircraft* 28 (3) (1991) 208–215.
- [4] D.S. Mandic, J.D. Jones, Adaptive active control of sound fields in elastic cylinders via vibration inputs, *AIAA Journal* 29 (10) (1991) 1552–1561.
- [5] C.R. Fuller, S.D. Snyder, C.H. Hansen, R.J. Silcox, Active control of interior noise in model aircraft fuselages using piezoceramic actuators, *AIAA Journal* 30 (11) (1992) 2613–2617.
- [6] J.Q. Sun, M.A. Norris, D.J. Rossetti, J.H. Highfill, Distributed piezoelectric actuators for shell interior noise control, *Journal of Vibration and Acoustics* 118 (1996) 676–681.
- [7] C.R. Fuller, R.A. Burdisso, A wavenumber domain approach to the active control of structure-borne sound, *Journal of Sound and Vibration* 148 (1991) 355–360.

- [8] B.T. Wang, The PVDF-based wave number domain sensing techniques for active sound radiation control from a simply supported beam, *Journal of Acoustic Society of America* 103 (1998) 1904–1915.
- [9] J.P. Maillard, C.R. Fuller, Advanced time domain wave-number sensing for structural acoustic systems. II. Active radiation control of a simply supported beam, *Journal of Acoustic Society of America* 95 (1994) 3262–3272.
- [10] J.P. Maillard, C.R. Fuller, Advanced time domain wave-number sensing for structural acoustic systems. III. Experiments on active broadband radiation control of a simply-supported plate, *Journal of Acoustic Society of America* 98 (1995) 2613–2621.
- [11] J.P. Maillard, C.R. Fuller, Active control of sound radiation from cylinders with piezoelectric actuators and structural acoustic sensing, *Journal of Sound and Vibration* 222 (3) (1999) 363–388.
- [12] S.J. Elliott, M.E. Johnson, Radiation modes and the active control of sound power, *Journal of Acoustical Society of America* 94 (4) (1993) 2194–2204.
- [13] S. Snyder, N. Tanaka, On feedforward active control of sound and vibration using error signals, *Journal of Acoustic Society of America* 94 (1993) 2181–2193.
- [14] B.S. Cazzolato, C.H. Hansen, Active control of sound transmission using structural error sensing, *Journal of Acoustic Society of America* 104 (1998) 2878–2889.
- [15] B.S. Cazzolato, C.H. Hansen, Structural sensing of sound transmission into a cavity for ASAC, *Proceedings of the Fifth International Congress of Sound and Vibration*, Adelaide, South Australia, Australia, December 1997, pp. 2391–2402.
- [16] D.S. Li, L. Cheng, C. Gosselin, Analysis of structural acoustic coupling of a cylindrical shell with an internal floor partition, *Journal of Sound and Vibration* 250 (2002) 903–921.
- [17] D.S. Li, L. Cheng, C.M. Gosselin, Optimal design of PZT actuators in active structural acoustic control of a cylindrical shell with a floor partition, *Journal of Sound and Vibration* 269 (2004) 569–588.
- [18] D.S. Li, L. Cheng, C.M. Gosselin, The design of structural acoustic sensors for active control of sound radiation into enclosures, *Smart Materials and Structures* 13 (2004) 371–384.
- [19] J.Q. Sun, S.M. Hirsch, V. Jayachandran, Sensor systems for global vibration and noise control, *Journal of Acoustical Society of America* 103 (3) (1998) 1504–1509.
- [20] J. Missaoui, L. Cheng, M.J. Richard, Free and forced vibration of a cylindrical shell with a floor partition, *Journal of Sound and Vibration* 190 (1) (1996) 21–40.
- [21] L. Cheng, Vibroacoustic modeling of mechanically coupled structures: artificial spring technique applied to light and heavy medium, *Shock and Vibration* 3 (1996) 193–200.
- [22] J. Missaoui, L. Cheng, A combined integro-modal approach for prediction acoustic properties of irregular-shaped cavities, *Journal of Acoustical Society of America* 101 (6) (1997) 3313–3321.
- [23] H.C. Lester, S. Lefebvre, Piezoelectric actuator models for active sound and vibration control of cylinder, *Journal of Intelligent Material Systems and Structures* Vol.4 (1993) 295–306.
- [24] H.S. Tzou, Y. Bao, V.B. Venkayya, Parametric study of segmented transducers laminated on cylindrical shells. Part 1: sensor patch, *Journal of Sound and Vibration* 197 (1996) 207–224.
- [25] B. Widrow, S.D. Stearns, *Adaptive Signal Processing*, Prentice-Hall Inc., NJ, 1985.